catalysts

MDPI

Article

Production of New Isoflavone Glucosides from Glycosylation of 8-Hydroxydaidzein by Glycosyltransferase from *Bacillus subtilis* ATCC 6633

Chien-Min Chiang [1], Tzi-Yuan Wang [2], Szu-Yi Yang [3], Jiumn-Yih Wu [4,*] and Te-Sheng Chang [3,*]

1 Department of Biotechnology, Chia Nan University of Pharmacy and Science, No. 60, Sec. 1, Erh-Jen Rd., Jen-Te District, Tainan 71710, Taiwan; cmchiang@mail.cnu.edu.tw
2 Biodiversity Research Center, Academia Sinica, Taipei 115, Taiwan; tziyuan@gmail.com
3 Department of Biological Sciences and Technology, National University of Tainan, Tainan 70005, Taiwan; szuyi08231995@gmail.com
4 Department of Food Science, National Quemoy University, Kinmen County 892, Taiwan
* Correspondence: wujy@nqu.edu.tw (J.-Y.W.); mozyme2001@gmail.com (T.-S.C.); Tel.: +886-8231-3310 (J.-Y.W.); Fax: +886-8231-3797 (J.-Y.W.); Tel./Fax: +886-6260-2137 (T.-S.C.)

Received: 24 August 2018; Accepted: 7 September 2018; Published: 10 September 2018

Abstract: 8-Hydroxydaidzein (8-OHDe) has been proven to possess some important bioactivities; however, the low aqueous solubility and stability of 8-OHDe limit its pharmaceutical and cosmeceutical applications. The present study focuses on glycosylation of 8-OHDe to improve its drawbacks in solubility and stability. According to the results of phylogenetic analysis with several identified flavonoid-catalyzing glycosyltransferases (GTs), three glycosyltransferase genes (*BsGT110*, *BsGT292* and *BsGT296*) from the genome of the *Bacillus subtilis* ATCC 6633 strain were cloned and expressed in *Escherichia coli*. The three BsGTs were then purified and the glycosylation activity determined toward 8-OHDe. The results showed that only *BsGT110* possesses glycosylation activity. The glycosylated metabolites were then isolated with preparative high-performance liquid chromatography and identified as two new isoflavone glucosides, 8-OHDe-7-*O*-β-glucoside and8-OHDe-8-*O*-β-glucoside, whose identity was confirmed by mass spectrometry and nuclear magnetic resonance spectroscopy. The aqueous solubility of 8-OHDe-7-*O*-β-glucoside and 8-OHDe-8-*O*-β-glucoside is 9.0- and 4.9-fold, respectively, higher than that of 8-OHDe. Moreover, more than 90% of the initial concentration of the two 8-OHDe glucoside derivatives remained after 96 h of incubation in 50 mM of Tris buffer at pH 8.0. In contrast, the concentration of 8-OHDe decreased to 0.8% of the initial concentration after 96 h of incubation. The two new isoflavone glucosides might have potential in pharmaceutical and cosmeceutical applications.

Keywords: *Bacillus*; glycosyltransferase; 8-hydroxydaidzein

1. Introduction

Daidzein and genistein, the major isoflavones found in soybean, have been under intensive investigation in the past few decades due to their potential roles in preventing certain hormone-dependent diseases [1]. In recent years, biotransformation of isoflavones using either wild-type or genetically-engineered microorganisms has also been of interest because the bioactivity of isoflavones dramatically alters after biotransformation. Among the various biotransformations of soy isoflavones, *ortho*-hydroxylation of soy isoflavones has become a subject of great interest because of the *ortho*-hydroxydaidzein and *ortho*-hydroxygenistein derivatives produced, which usually possess higher bioactivities compared with those of the precursors, daidzein and genistein [2].

8-Hydroxydaidzein (8-OHDe) is one of the *ortho*-hydroxydaidzein derivatives. The compound can be produced from biotransformation of daidzein by either wild *Aspergillus oryzae* [3–5], genetically-engineered *Pichia pastoris* [6] or *Escherichia coli* [7,8]. Multiple bioactivities related to 8-OHDe have been reported, including anti-cancer [9], suppression of multidrug resistance [10], anti-tyrosinase [11,12], skin whitening [13,14], anti-aldose reductase [15] and the newly-found anti-inflammatory activity [16,17].

Although 8-OHDe has been identified with many bioactivities, some drawbacks (including low aqueous solubility and stability) limit isoflavone's application in pharmaceuticals and cosmeceuticals [18]. To improve the drawbacks of 8-OHDe, biotransformation through whole cells or enzyme biocatalysts into 8-OHDe derivatives is a promising strategy. Among various biotransformations, glycosylation, the attachment of a bulky sugar group to the precursor molecules, could improve the chemical stability and aqueous solubility of natural compounds. The aqueous solubility of the corresponding 7-*O*-glucoside of soy isoflavones is improved about 30-fold [19]. Increasing the aqueous solubility and stability could expand applications of the compounds in advance. Therefore, in the present study, we are interested in investigating the glycosyl-biotransformation of 8-OHDe.

Glycosylation is a common modification reaction in the biosynthesis of natural compounds. Generally, glycosylation is catalyzed by glycosyltransferases (GTs, EC 2.4.x.y), which transfer sugar moieties from the activated donor molecules to specific acceptor molecules [20–22]. Our previous studies found that *Bacillus subtilis* ATCC 6633 could biotransform antcin K, which is a major ergostane triterpenoid from the fruiting bodies of *Antrodia cinnamomea*, to its glucoside derivatives [23]. In the present study, the *B. subtilis* strain was found to biotransform 8-OHDe. To identify the biotransformation in advance, three GT genes were cloned from the *B. subtilis* strain and overexpressed in *Escherichia coli*. Then, the biotransformation activity of the three purified GT enzymes toward 8-OHDe was determined. The biotransformed metabolites by one positive-active enzyme were isolated and identified. Finally, the aqueous solubility and stability of the 8-OHDe glucoside derivatives were determined.

2. Results and Discussion

2.1. Confirming Biotransformation of 8-OHDe by Bacillus subtilis *ATCC 6633*

Our previous studies showed that *B. subtilis* ATCC 6633 could biotransform the ergostane triterpenoid antcin K to its glucoside derivatives [23]. To confirm whether *B. subtilis* ATCC 6633 could also biotransform 8-OHDe, the bacterium was cultivated in broth with 8-OHDe, and the fermentation broth was analyzed using ultra-performance liquid chromatography (UPLC).

Figure 1 shows the UPLC analysis of the initial (dashed line) and 24-h (solid line) fermentation broths of the strain *B. subtilis* ATCC 6633 fed with 8-OHDe. In the figure, 8-OHDe appears at the retention time (RT) of 5.1 min. After 24 h of fermentation, the peak of the precursor decreases, while several new peaks with RTs of between 3 and 4 min appear. To confirm whether the new peaks are from biotransformation of 8-OHDe, biotransformation was conducted in the absence of 8-OHDe. The results showed that the new peaks did not appear at 24 h of the fermentation broth of the strain in the absence of 8-OHDe (Figure S1). Thus, it was concluded that 8-OHDe was biotransformed by the strain *B. subtilis* ATCC 6633.

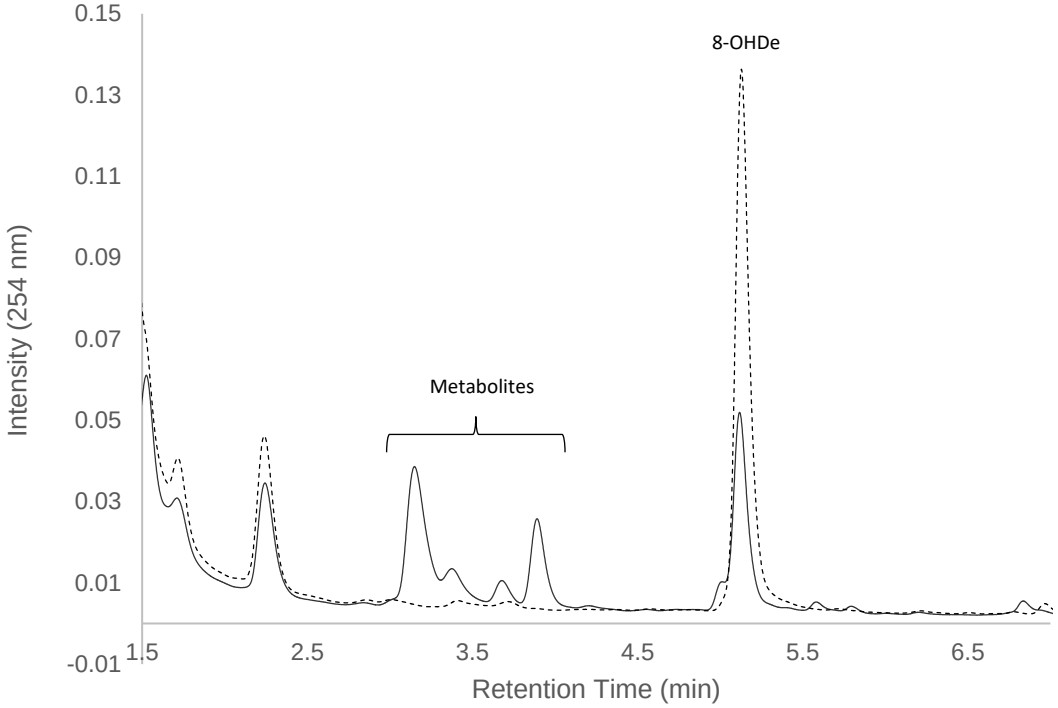

Figure 1. Biotransformation of 8-hydroxydaidzein (8-OHDe) by *B. subtilis* ATCC 6633. The strain was cultivated in modified glucose nutrient (MGN) media containing 0.02 mg/mL of 8-OHDe. The initial (dashed line) and 24-h (solid line) cultivations of the fermentation broth were analyzed with UPLC. The UPLC operation conditions are described in the Materials and Methods.

2.2. *Phylogenetic Analysis of GTs from* B. subtilis *ATCC 6633*

Although *B. subtilis* ATCC 6633 has been proven to biotransform the ergostane triterpenoid antcin K [23] and 8-OHDe (Figure 1), biotransformation by using whole cells as biocatalysts usually has lower efficiency than that by using purified enzyme, which can be produced through genetic engineering. Thus, cloning of the putative genes encoding the catalytic enzymes in the biotransformation is a worthy strategy. According to the genome data of *B. subtilis* ATCC 6633 (GenBank BioProject Accession No. PRJNA43011), there are 28 GTs annotated in the genome. To clone the GT genes from *B. subtilis* ATCC 6633 responsible for the biotransformation of 8-OHDe, phylogenetic analysis of the annotated GTs from *B. subtilis* ATCC 6633 was compared with known bacterial GTs, which have been proven to possess glycosylation activity toward flavonoids. The characterized bacterial glycosyltransferases included BlYjiC (AAU40842) from *B. licheniformis* ATCC 14580 [24], BsYjiC (NP_389104) from *B. subtilis* 168 [25,26], BcGT-1 (AAS41089) and BcGT-3 (AAS41737) from *B. cereus* ATCC 10987 [27,28], OleD (ABA42119) from *Streptomyces antibioticus* [29] and XcGT-2 (AAM41712) from *Xanthomonas campestris* pv. *campestris* ATCC 33913 [30]. The results are shown in Figure 2. According to the results of the phylogenetic analysis, all tested six identified flavonoid-catalyzing GTs (gray background in Figure 2) were clustered into one group (Figure 2). Among the 28 BsGTs, only *BsGT110* was included in the group. At the same time, *BsGT292* and *BsGT296* were close to the group. Thus, the three GTs, *BsGT110* (GenBank Protein Accession No. WP_003220110), *BsGT292* (GenBank Protein Accession No. WP_032727292) and *BsGT296* (GenBank Protein Accession No. WP_003219296; bold text in Figure 2), were selected for further functional assay.

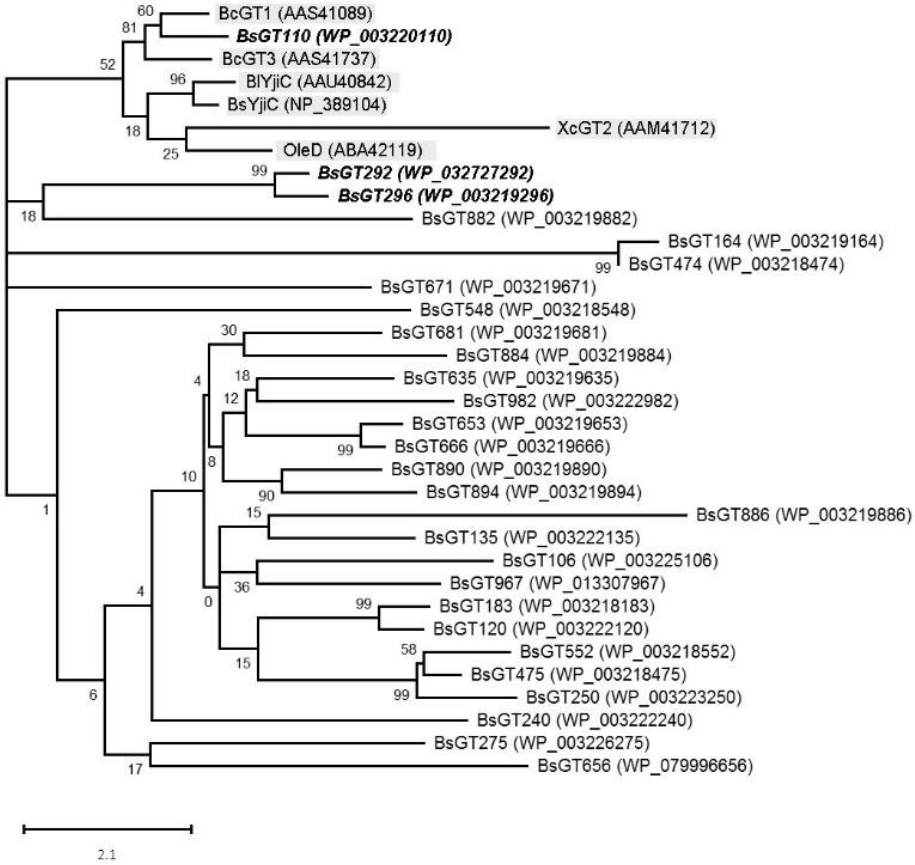

Figure 2. Unrooted phylogenetic analysis of glycosyltransferase genes by using the maximum likelihood method. The tree with the highest log likelihood (−19,549.15) is shown based on the general reversible mitochondrial model [31]. The percentage of trees in which the associated taxa clustered together is shown next to the branches. Initial trees for the heuristic search were obtained automatically by applying the neighbor-join and BioNJ algorithms to a matrix of pairwise distances estimated using a JTT model and then selecting the topology with the superior log likelihood value. The rate variation model allowed for some sites to be evolutionarily invariable ([+I], 0.00% sites). The tree is drawn to scale, with branch lengths measured in the number of subsstitutions per site. The analysis involved 34 protein sequences. All positions with less than 95% site coverage were eliminated. That is, fewer than 5% alignment gaps, missing data and ambiguous bases were allowed at any position. There were a total of 210 positions in the final dataset. Evolutionary analyses were conducted in Molecular Evolutionary Genetics Analysis (MEGA X) across computing platforms (Version 10.0.4, Center for Evolutionary Functional Genomics, The Biodesign Institute, Arizona State University, Tempe, AZ, USA, 1993–2018) [32].

2.3. Cloning, Overexpression, Purification and Activity Assay of BsGTs from B. subtilis *ATCC 6633 in E. coli*

To identify which enzyme catalyzed the biotransformation, the three BsGT genes were cloned into a pETDuet-1 expression vector (Figure 3a). The recombinant BsGT gene in recombinant *E. coli* was overexpressed by induction with 0.2 mM of isopropyl β-D-1-thiogalactopyranoside (IPTG), and the protein produced was purified with Ni^{2+} chelate affinity chromatography. Figure 3b shows the sodium dodecyl sulfate polyacrylamide gel electrophoresis (SDS-PAGE) analysis of the overexpressed and purified *BsGT110*, while the SDS-PAGE analysis of purified *BsGT292* and *BsGT296* is in Figure S2.

The purified enzymes were incubated with uridine diphosphate (UDP)-glucose and the precursor 8-OHDe to confirm their biotransformation activity toward 8-OHDe. The results showed that only *BsGT110* has biotransformation activity toward 8-OHDe (Figure 4), while neither purified *BsGT292*, nor *BsGT296* showed the activity (Figure S3). The result was consistent with the phylogenetic analysis results (Figure 2), where only *BsGT110* was clustered with the group of flavonoid-catalyzing GTs.

In addition, the RTs of the two biotransformation metabolites (Figure 4), 3.7 min and 3.9 min for Compound (**1**) and Compound (**2**), respectively, were similar to some of the new peaks in the 8-OHDe biotransformation by the strain *B. subtilis* ATCC 6633 (Figure 1). The results imply that *BsGT110* is one of the corresponding enzymes catalyzing 8-OHDe during the biotransformation of 8-OHDe by the strain *B. subtilis* ATCC 6633.

By comparing the results of the biotransformations using whole cells (Figure 1) and the purified *BsGT110* (Figure 4), it is obvious that biotransformation products using the purified *BsGT110* (Compound (**1**) and Compound (**2**) in Figure 4) were more specific than those using the whole cells (metabolites between RT 3 and 4 min in Figure 1). Moreover, the catalyzing efficiency using the purified *BsGT110* (reaction time of 30 min in Figure 4) was higher than that using whole cells (reaction time of 24 h in Figure 1). Therefore, biotransformation by using the purified *BsGT110* as biocatalysts has higher efficiency and specificity than those by using whole cells.

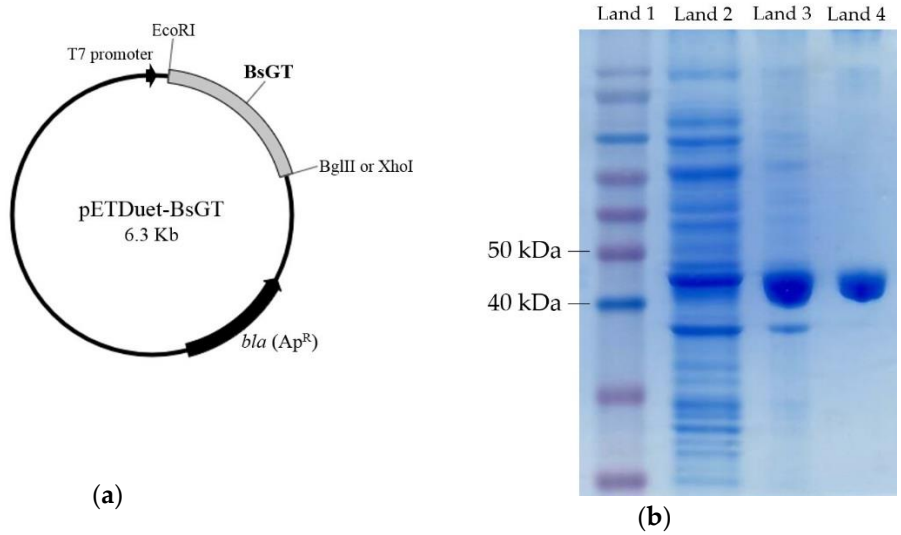

Figure 3. Expression and purification of the BsGTs from *B. subtilis* ATCC 6633 in *E. coli*. (**a**) Diagram of the recombinant expression plasmid; (**b**) SDS-PAGE analysis of expressed and purified proteins from recombinant *E. coli* harboring pETDuet-*BsGT110*. Lane 1: molecular marker; Lane 2: total protein before induction; Lane 3: total protein after 20 h induction; Lane 4: purified protein.

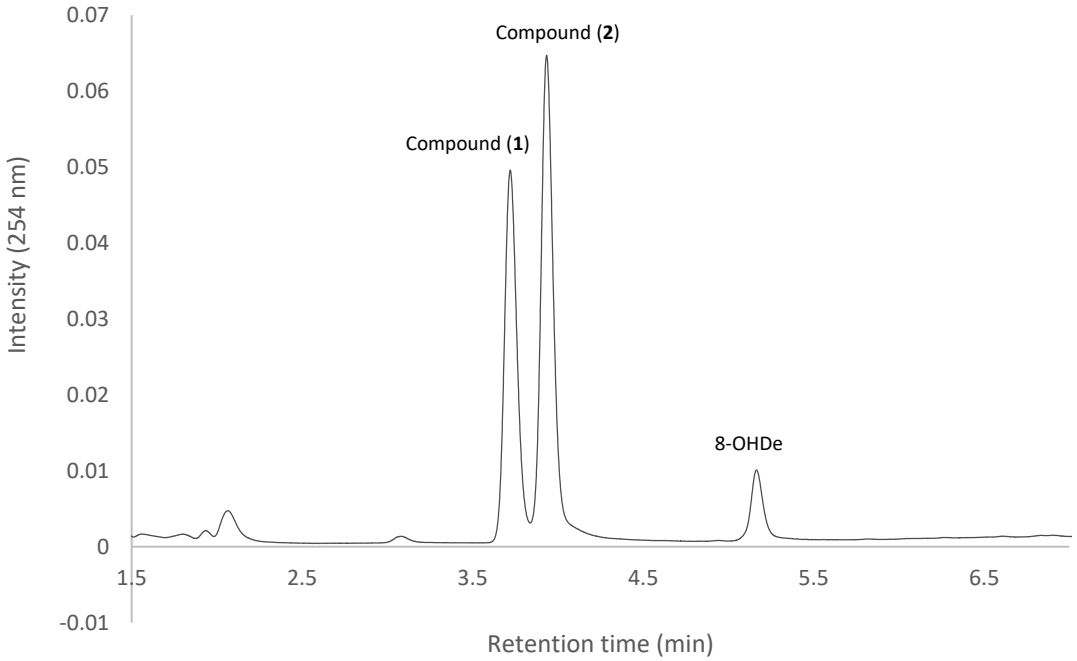

Figure 4. Biotransformation of 8-OHDe by the purified *BsGT110*. Two micrograms of the purified enzyme were incubated with 0.4 mM uridine diphosphate (UDP)-glucose and 0.02 mg/mL of 8-OHDe in the presence of 50 mM Tris at pH 8.0 and 10 mM of $MgCl_2$ at 40 °C for 30 min. After the reaction, the mixtures were analyzed with ultra-performance liquid chromatography (UPLC). The UPLC operation conditions are described in the Materials and Methods.

2.4. Optimal Catalyzing Conditions for BsGT110

To determine the optimal catalyzing condition, the activity of *BsGT110* at different pH values, temperatures and metal ions was examined. The results are shown in Figure 5. The enzyme activity was very sensitive to pH, and the enzyme activity at pH 7.0 was nearly 3–4-fold higher than that at pH 8.0 and pH 6.0. However, the enzyme activity was insensitive to temperature, and the enzyme activity was not significantly different between 30 °C and 50 °C. In addition, the enzyme favored Ca^{2+} as its cofactor. In the presence of Ca^{2+}, the enzyme activity was 1.8-fold higher than that at Mg^{2+} or none. It is known that GTs utilize divalent metal ion cofactors such as Mn^{2+} and Mg^{2+}. However, Li et al. found that the activity of the GT from *Bacillus circulans* was enhanced by Ca^{2+} due to an additional calcium-binding site in the structure [33]. Whether *BsGT110* favored Ca^{2+} as its cofactor due to an additional calcium-binding site needs to be studied in the future. From the results, the optimal catalyzing conditions for *BsGT110* are at 40 °C, pH 7.0 with 10 mM of Ca^{2+}.

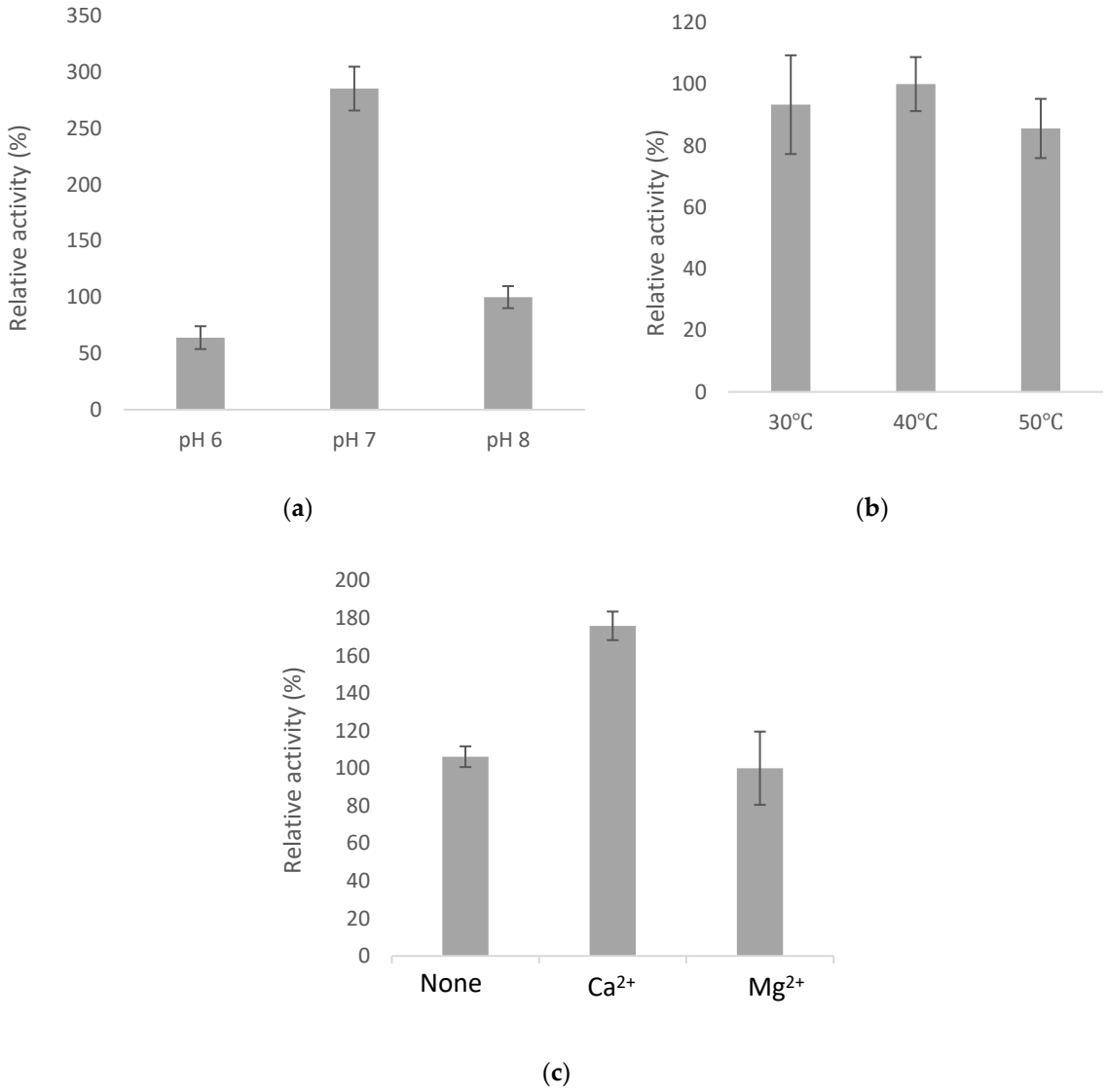

Figure 5. Effects of pH (**a**), temperature (**b**) and metal ion (**c**) on *BsGT110* activity. A standard condition was set as 2 μg of the purified *BsGT110*, 1 mg/mL of 8-OHDe, 10 mM of $MgCl_2$ and 10 mM of UDP-glucose in 50 mM of Tris at pH 8.0 and 40 °C. To determine the optimal reaction condition, the pH, temperature or metal ion in the standard condition was replaced by the tested condition. Relative activity was obtained by dividing the area of the summation of the two product peaks, Compound (**1**) and Compound (**2**), of the reaction in the UPLC profile by that of the reaction at the standard condition. The mean (n = 3) is shown, and the standard deviations are represented by error bars.

2.5. Substrate Specificity of BsGT110

To study the substrate specificity of *BsGT110*, another three *ortho*-hydroxyisoflavones (3′-hydroxydaidzein, 3′-OHDe; 3′-hydroxygenistein, 3′-OHGe; 6′-hydroxydaidzein, 6-OHDe) were used in the biotransformation assays by *BsGT110*. The result is shown in Figure 6 and reveals that *BsGT110* could also catalyze all the tested *ortho*-hydroxyisoflavones. However, unlike two major metabolites, Compound (**1**) and Compound (**2**), produced in the biotransformation of 8-OHDe by *BsGT110* (Figure 4), only one major metabolite appeared in the biotransformations of either 3′-OHDe, 3′-OHGe or 6-OHDe by *BsGT110* (Figure 6). Due to very low amounts of the three *ortho*-hydroxyisoflavones, the biotransformation metabolites from these biotransformations were not identified in advance. In addition, among the *ortho*-hydroxyisoflavones in the present study, including

3′-OHDe, 3′-OHGe, 6-OHDe and 8-OHDe, only 8-OHDe has been approved to possess bioactivity in human volunteers [13,14]. Therefore, 8-OHDe was used as a substrate for the following study.

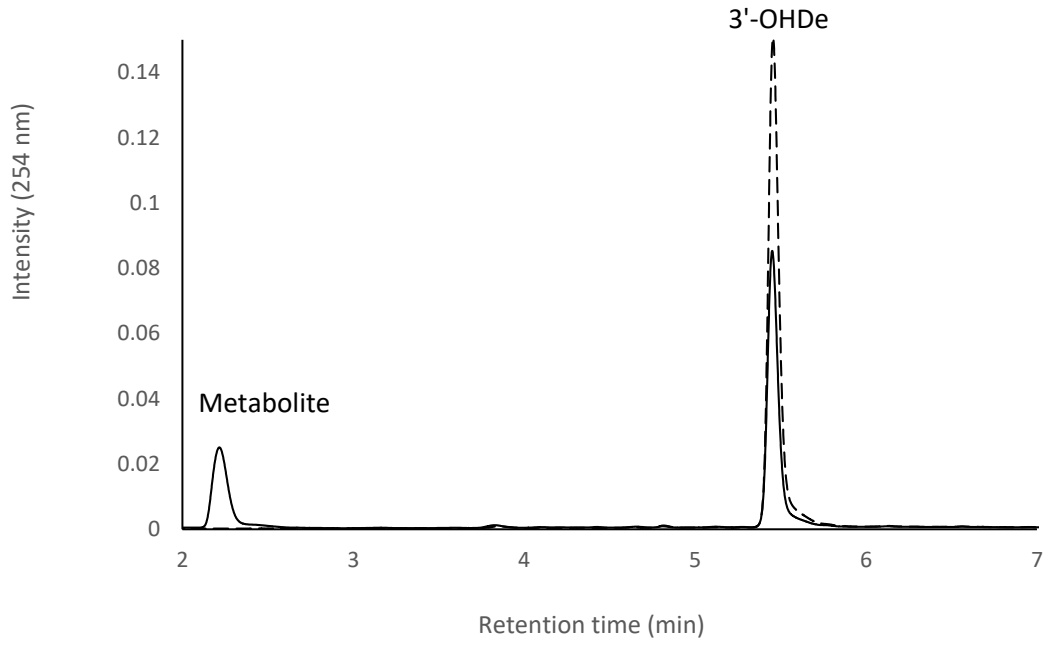

(**a**)

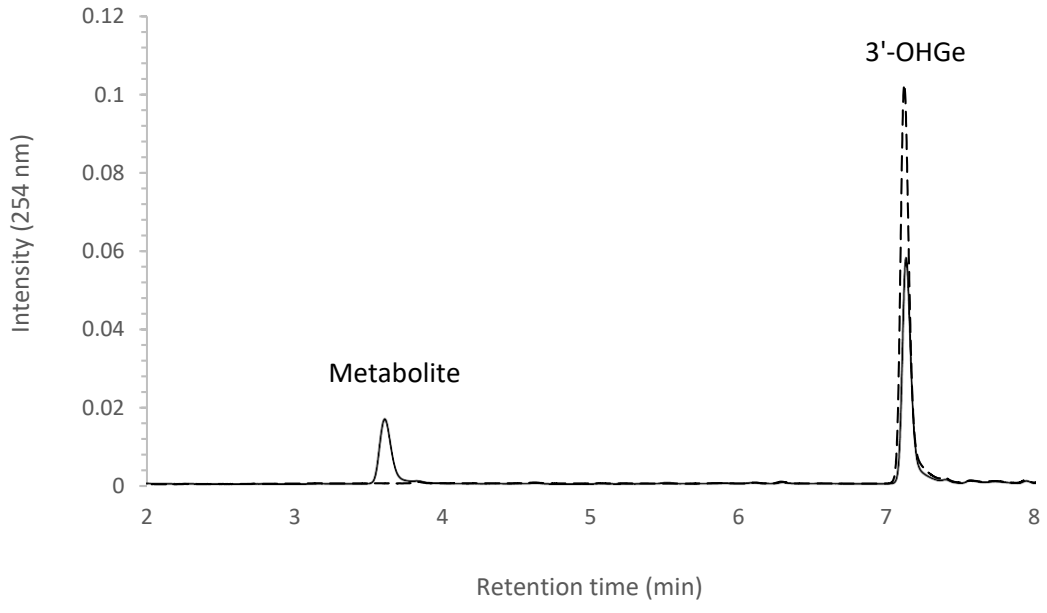

(**b**)

Figure 6. *Cont.*

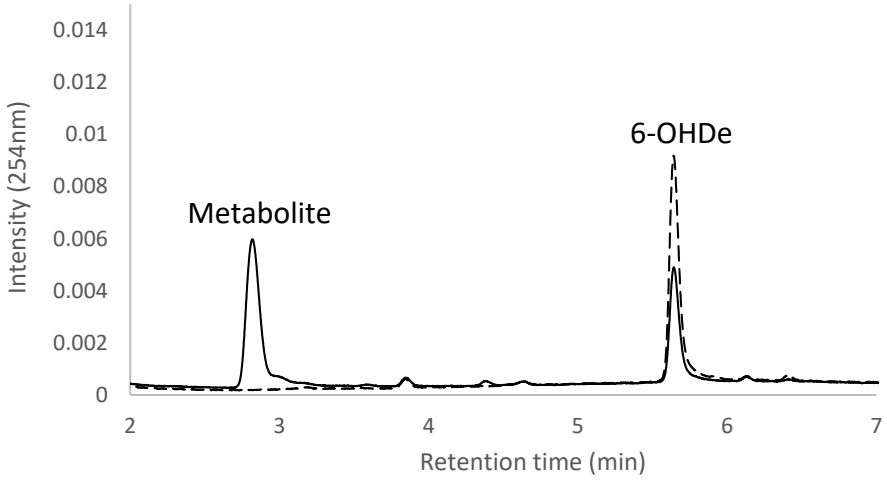

(c)

Figure 6. Biotransformation of 3′-hydroxydaidzein (3′-OHDe) (**a**), 3′-hydroxygenistein (3′-OHGe) (**b**) and 6′-hydroxydaidzein (6-OHDe) (**c**) by the purified *BsGT110*. Two micrograms of the purified enzyme were incubated with 0.4 mM uridine diphosphate (UDP)-glucose and 0.02 mg/mL of 3′-OHDe (a), 3′-OHGe (b) or 0.005 mg/mL of 6-OHDe (c) in the presence of 50 mM phosphate buffer at pH 7.0 and 10 mM of $CaCl_2$ at 40 °C for 30 min. Before (dashed line) and after (solid line) the reaction, the mixtures were analyzed with ultra-performance liquid chromatography (UPLC). The UPLC operation conditions are described in the Materials and Methods.

2.6. Stability of BsGT110

To study the stability of *BsGT110*, *BsGT110* was incubated at different temperatures for 1 h or was freeze-dried once, and then, the activity of the treated *BsGT110* was determined. The result is shown in Figure 7. The enzyme was not stable above 40 °C for 1 h, while the enzyme was stable after freeze-drying.

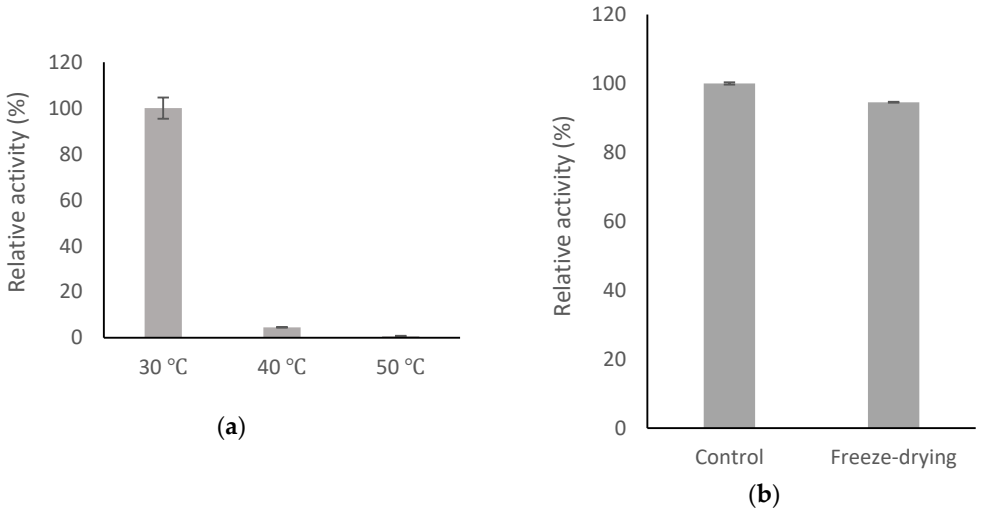

Figure 7. Stability of *BsGT110* at different temperatures (**a**) and with freeze-drying (**b**). Two micrograms of the purified *BsGT110* were pre-incubated at the tested temperature for 1 h or freeze-dried before conduction of the activity assay. A standard condition was set as 2 μg of the purified *BsGT110*, 1 mg/mL of 8-OHDe, 10 mM of $CaCl_2$ and 10 mM of UDP-glucose in 50 mM of phosphate at pH 7.0 and 40 °C. Relative activity was obtained by dividing the area of the summation of the two product peaks, Compound (**1**) and Compound (**2**), of the reaction in the UPLC profile by that of the reaction at the standard condition. The mean (n = 3) is shown, and the standard deviations are represented by error bars.

2.7. Isolation and Identification of Biotransformation Metabolites

To resolve the chemical structures of the metabolites, the biotransformation was scaled up at the optimal condition, and the two metabolites were purified with preparative high-performance liquid chromatography (HPLC). From a 40-mL reaction mixture containing 1 mg/mL of 8-OHDe, 10 mM of UDP-glucose, 10 mM of $CaCl_2$ and 50 mM of phosphate buffer at pH 7.0, 17.4 mg and 24.5 mg of Compound (**1**) and Compound (**2**) were isolated. Both compounds showed an $[M^-H]^-$ ion peak at *m*/*z*: 431.23 in the electrospray ionization mass (ESI-MS) spectrum corresponding to the molecular formula $C_{21}H_{20}O_{10}$. Then, ^1H and ^{13}C nuclear magnetic resonance (NMR), including distortionless enhancement by polarization transfer (DEPT), heteronuclear single quantum coherence (HSQC), heteronuclear multiple bond connectivity (HMBC), correlation spectroscopy (COSY) and nuclear Overhauser effect spectroscopy (NOESY) spectra, were obtained, and the ^1H- and ^{13}C-NMR signal assignments were conducted accordingly (shown in Figures S4–S17). In both compounds, in addition to the signals of the 8-OHDe moiety, which were confirmed by HMBC spectra (full assignments of both compounds are listed in Table S1), seven proton (from 3.18 to 4.93 ppm) and six carbon (from 60 to 105 ppm) signals corresponding to the glucose moiety structure were observed. The anomeric proton signal at δ 4.91 (J = 7.6 Hz) and 4.93 (J = 7.7 Hz) in the ^1H-NMR spectra of Compounds (**1**) and (**2**), respectively, indicated the β-configuration for the glucopyranosyl moiety. The cross peak of H-1″ with C-7 (4.91/149.0 ppm) in the HMBC spectrum, as well as the cross peak of H-1″ with H-6 (4.91/ 7.30 ppm) in the NOESY spectrum demonstrated that the structure of Compound (**1**) was 8-OHDe-7-*O*-β-glucoside. The cross peaks of H-1″ with C-8 (4.93/131.9 ppm) and H-6 with C-8 (7.02/131.9 ppm) in the HMBC spectrum demonstrated that the structure of Compound (**2**) was 8-OHDe-8-*O*-β-glucoside. The key HMBC and NOESY correlations of Compounds (**1**) and (**2**) and the illustration of the biotransformation process of 8-OHDe by *BsGT110* are shown in Figure 8.

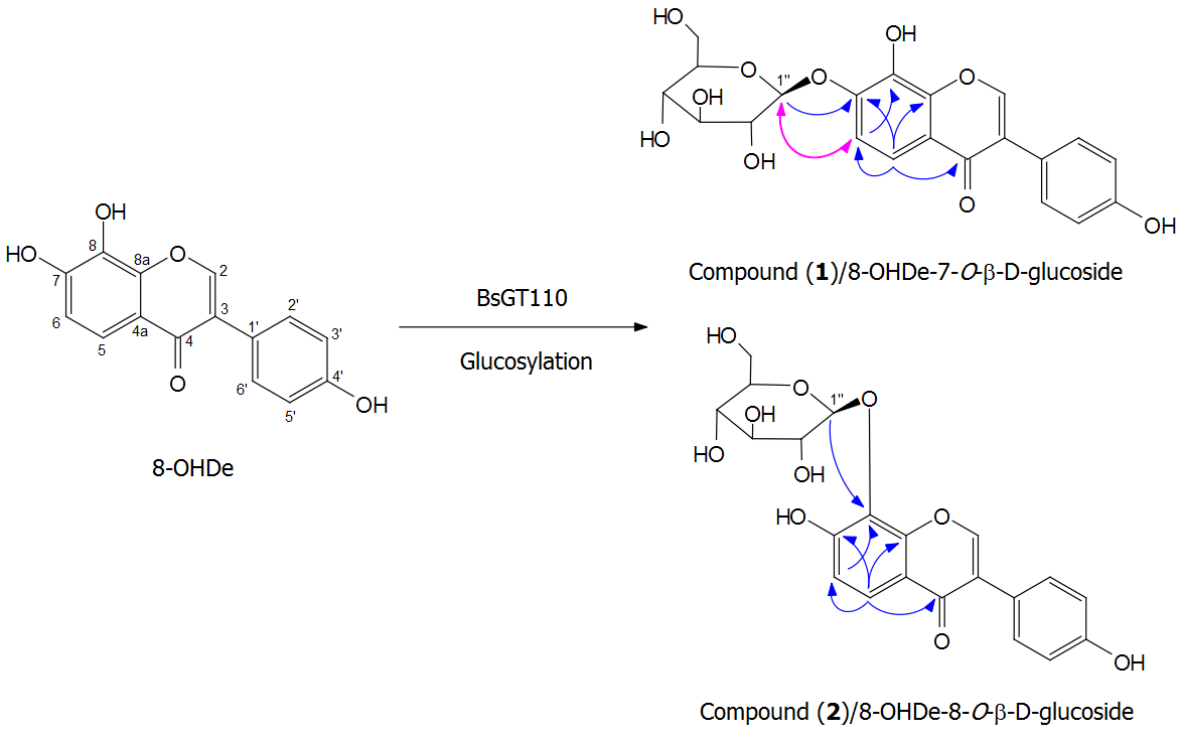

Figure 8. Biotransformation process of 8-OHDe by *BsGT110*. The key HMBC (H–C, blue arrows) and NOESY (pink arrows) correlations of Compound (**1**) and Compound (**2**).

2.8. Determination of Aqueous Solubility of 8-OHDe and Its Glucosides

The aqueous solubility of 8-OHDe and the two 8-OHDe glucoside derivatives was examined and is summarized in Table 1. The results revealed that the aqueous solubility of 8-OHDe-7-*O*-β-glucoside and 8-OHDe-8-*O*-β-glucoside was 9.0- and 4.9-fold, respectively, higher than that of 8-OHDe.

Table 1. Aqueous solubility of 8-OHDe and its glucoside derivatives.

Compound	Aqueous Solubility (mg/L)	Fold [1]
8-OHDe	51.3	1
8-OHDe-7-*O*-β-glucoside	462.0	9.0
8-OHDe-8-*O*-β-glucoside	251.1	4.9

[1] The fold of aqueous solubility of 8-OHDe glucoside derivatives is expressed relative to that of 8-OHDe, normalized to 1.

2.9. Determination of Stability of 8-OHDe and Its Glucosides

8-OHDe has been proven to be unstable in alkaline solution [18]. To determine the stability of 8-OHDe and its glucosides, the tested compounds were added in 50 mM of Tris at pH 8.0 and 20 °C. The residues of the compounds were monitored with UPLC at different time intervals. The results are shown in Figure 9. The amount of 8-OHDe decreased to 38% of the initial concentration after 24 h and decreased to 0.8% of the initial concentration after 96 h. In contrast, more than 90% of the two 8-OHDe glucoside derivatives remained after 96 h of incubation. The results revealed that the two 8-OHDe glucoside derivatives were much more stable than 8-OHDe in the aqueous solution.

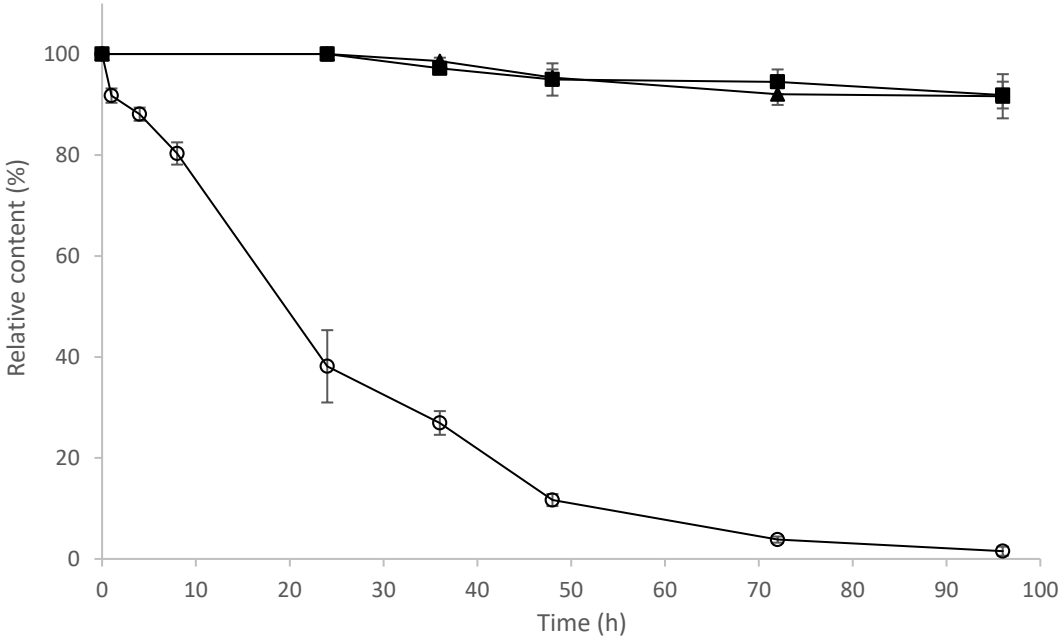

Figure 9. Stability of 8-OHDe and its glucosides. One milligram per milliliter of the tested compound was dissolved in 50 mM of Tris buffer at pH 8.0 and stored at 20 °C for 96 h. During the storage time, samples were taken out for the UPLC analysis at the determined interval times. The mean (n = 3) is shown, and the standard deviations are represented by error bars.

8-OHDe has been proven to possess multiple bioactivities; especially, 8-OHDe has been proven for its skin-whitening activity in vivo in the skin of mice and human volunteers [13,14]. Some skin-whitening agents maintain skin-whitening activity after glycosylation. For examples, ascorbic acid and hydroquinone are famous skin-whitening agents. Their glucoside derivatives, ascorbic acid 2-glucosdie (AA2G) and arbutin (hydroquinone-glucoside), possess potent skin-whitening activity and are the most well-known

skin-whitening agents used in cosmetic markets nowadays. In our previous study, we found that *ortho*-hydroxyisoflavone glucosides possessed skin-whitening activity in vivo in the skin of mice [34]. Therefore, the 8-OHDe glucosides in the present study might have skin-whitening activity. The experiments to evaluate the in vivo skin-whitening activity in the mice skin of the 8-OHDe glucosides in the present study were conducting in our laboratory.

3. Materials and Methods

3.1. Microorganisms, Animal Cells and Chemicals

Bacillus subtilis ATCC 6633 (BCRC 10447) was purchased from the Bioresources Collection and Research Center (BCRC, Food Industry Research and Development Institute, Hsinchu, Taiwan). 8-OHDe was prepared according to Wu et al.'s [4] method. 3′-OHDe and 3′-OHGe were prepared according to our previous study [35]. 6-OHDe was purchased from Sigma (St. Louis, MO, USA). UDP-glucose was obtained from Cayman Chemical (Ann Arbor, MI, USA). All the materials needed for polymerase chain reaction (PCR), including primers, deoxyribonucleotide triphosphate and Taq DNA polymerase, were purchased from MDBio (Taipei, Taiwan). pETDuet-1 plasmid was purchased from Novagen (Madison, WI, USA). Restriction enzymes and DNA ligase were obtained from New England Biolabs (Ipswich, MA, USA). The other reagents and solvents used were of high quality and were purchased from commercially available sources.

3.2. Identification of Bacteria B. subtilis *ATCC 6633 with Biotransformation Activity*

Bacillus subtilis ATCC 6633 was cultivated in a 250-mL baffled Erlenmeyer flask containing 20 mL of a modified glucose-nutrient (MGN) medium (5 g/L of peptone, yeast extract, K_2HPO_4 and NaCl; 20 g/L of glucose) and 20 mg/L of 8-OHDe. After cultivation at 180 rpm, 28 °C for 24 h, 1 mL of the culture was then mixed with an equal volume of methanol. The cell debris was removed by centrifugation at 10,000× *g* for 10 min. The supernatant from the extracted broth was assayed with UPLC to measure the biotransformation activity.

3.3. UPLC Analysis

The UPLC system (Acquity UPLC H-Class, Waters, Milford, MA, USA) was equipped with an analytic C18 reversed-phase column (Acquity UPLC BEH C18, 1.7 μm, 2.1 i.d. × 100 mm, Waters, Milford, MA, USA). The operation conditions contained a gradient elution using water (A) containing 1% (v/v) acetic acid and methanol (B) with a linear gradient for 7 min with 35% to 80% B at a flow rate of 0.2 mL/min, an injection volume of 0.2 μL and absorbance detection at 254 nm.

3.4. Phylogenetic Analysis of BsGTs

The unrooted phylogenetic tree of the candidate genes was constructed with the maximum likelihood method, using Molecular Evolutionary Genetics Analysis (MEGA X) software (Version 10.0.4, Center for Evolutionary Functional Genomics, The Biodesign Institute, Arizona State University, Tempe, AZ, USA, 1993–2018) [32] with 500 bootstrap replications, the mtREV24+I model [31] and partial deletion.

3.5. Expression and Purification of UGT398 and UGT489

The genomic DNA of *B. subtilis* ATCC 6633 was isolated using the commercial kit Geno *Plus*™ (Viogene, Taipei, Taiwan). The three GT target genes, *BsGT110* (GenBank Protein Accession No. WP_003220110), *BsGT292* (GenBank Protein Accession No. WP_032727292) and *BsGT296* (GenBank Protein Accession No. WP_003219296), were amplified from the genomic DNA with PCR with the following primer sets: forward: 5′-CGC GAA TTC ggc taa tgt att aat gat cgg tt-3′; reverse: 5′-CGC AGA TCT tta tgc gtt ggc tga ttg agt tt-3′ for *BsGT110*; forward: 5′-CGC GAA TTC gat gaa gct tgc ctt tat ctg tac ag-3′; reverse: 5′-CGC CTC GAG tta tga ttt ggc ttt cac aaa aag c-3′ for *BsGT292*; forward:

5′-CGC GAA TTC Gat gaa aat agc act gat cgc cac ag-3′; reverse: 5′-CGC CTC GAG cta tct gtt ctt ctc ata cac gct g-3′ for BsGT296. Restriction enzyme-recognizing sites were designed at the forward primer (EcoRI, GAATTC) for the three BsGTs and the reverse primer (BglII, AGATCT) for *BsGT110* and (XhoI, CTCGAG) for *BsGT 292* and *BsGT296*. The amplified *BsGT* genes were subcloned into the corresponding sites of the pETDuet-1™ vector to obtain the expression vector pETDuet-BsGT (Figure 3a). In the cloning strategy, the N-terminal fusion with His-tag would allow the expressed proteins to be purified with Ni^{2+} chelate affinity chromatography. The expression vectors were transformed into *E. coli* BL21 (DE3) via electroporation to obtain the recombinant *E. coli*.

The recombinant *E. coli* was cultivated in 150 mL of Luria–Bertani (LB) medium containing 50 μg/mL of ampicillin with 200 rpm shaking at 37 °C. When the optical density at 600 nm reached 0.6, 0.2 mM IPTG was added to induce expression of the *BsGT* genes. The cells were continuously cultured in an incubator at 18 °C for another 20 h. At the end of the cultivation, the cells were harvested by centrifugation at 5000 rpm and 4 °C and washed once with 100 mL of phosphate saline buffer (PBS, 50 mM phosphate pH 6.8 and 100 mM NaCl). The cells were resuspended in 5 mL of PBS containing 25 mM of imidazole and broken by sonication at 4 °C. Cell debris was removed by centrifugation at 17,000× *g* for 30 min 4 °C. The supernatant containing the recombinant UGTs was applied on a Ni^{2+} chelate affinity column (10 i.d. × 50 mm, Ni Sepharose 6 Fast Flow, GE Healthcare, Chicago, IL, USA). After washing with 20 mL of PBS containing 25 mM of imidazole, the bound proteins were eluted with 15 mL of PBS containing 250 mM of imidazole. The elute protein was dialyzed twice against 50 mM Tris pH 8.0 and 100 mM of NaCl and then concentrated using Macrosep 10K centrifugal filters (Pall, Ann Arbor, MI, USA). The purity and molecular weights of the purified UGTs were analyzed with SDS-PAGE. The protein concentration was measured with the Bradford method with bovine serum albumin as the standard. The final purified proteins were stored at −80 °C in the presence of 50% of glycerol for use.

3.6. In Vitro Biotransformation Assay

The in vitro biotransformation was conducted with the purified BsGTs. The reaction (1 mL) containing 2 μg of the tested enzyme, 0.02 mg/mL of 8-OHDe, 0.4 mM of UDP-glucose, 10 mM of $MgCl_2$ and 50 mM of Tris at pH 8.0 was carried out at 40 °C for 30 min. After the reaction, the mixture was stopped by adding an equal volume of methanol and analyzed with UPLC. To determine the optimal condition, a standard condition was set as 2 μg of the purified *BsGT110*, 1 mg/mL of 8-OHDe, 10 mM of $MgCl_2$ and 10 mM of UDP-glucose at 50 mM of Tris at pH 8.0 and 40 °C, and the pH, temperature or metal ion in the standard condition was replaced by the tested condition. For pH testing, phosphate buffer (pH 6.0 and 7.0) and Tris buffer (pH 8.0) were used. For metal ion testing, 10 mM of either $MgCl_2$ or $CaCl_2$ were used. Relative activity was obtained by dividing the area of the summation of the two product peaks, Compound (**1**) and Compound (**2**), of the reaction in the UPLC profile by that of the reaction at the standard condition.

3.7. Scale-Up, Isolation and Identification of the Biotransformation Product

To purify the biotransformation metabolites, the reaction was scaled up to a 40-mL reaction mixture containing 20 μg of the purified *BsGT110*, 1 mg/mL of 8-OHDe, 10 mM of UDP-glucose, 10 mM of $CaCl_2$ and 50 mM of phosphate buffer at pH 7.0. After reaction at 40 °C for 30 min, 40 mL of methanol were added to stop the reaction. After being filtrated through a 0.2-μm nylon membrane, the mixture was injected into a preparative YoungLin HPLC system (YL9100, YL Instrument, Gyeonggi-do, Korea). The system was equipped with a preparative C18 reversed-phase column (Inertsil, 10 μm, 20.0 i.d. × 250 mm, ODS 3, GL Sciences, Eindhoven, The Netherlands). The operational conditions for the preparative HPLC analysis were the same as those in the UPLC analysis. The elution corresponding to the peak of the metabolite in the UPLC analysis was collected, concentrated under vacuum and then lyophilized. Finally, 17.4 mg and 24.5 mg of Compound (**1**) and Compound (**2**) were isolated, and the structures of the compounds were confirmed with NMR and mass spectral analysis. The mass

analysis was performed on a Finnigan LCQ Duo mass spectrometer (ThermoQuest Corp., San Jose, CA, USA) with electrospray ionization (ESI). ^{1}H- and ^{13}C-NMR, DEPT, HSQC, HMBC, COSY and NOESY spectra were recorded on a Bruker AV-700 NMR spectrometer (Bruker Corp., Billerica, MA, USA) at ambient temperature. Standard pulse sequences and parameters were used for the NMR experiments, and all chemical shifts were reported in parts per million (ppm, δ).

3.8. Determination of Solubility

Aqueous solubility of 8-OHDe and its glucoside derivatives was examined as follows. Each compound was vortexed in d.d. H_2O for 1 h at 25 °C. The mixture was centrifuged at 10,000× *g* for 30 min at 25 °C and analyzed with UPLC. The concentrations of the tested compounds were determined based on their peak areas using calibration curves prepared with UPLC analyses of authentic samples.

3.9. Determination of Stability

A stock of 8-OHDe or its glucosides (100 mg/mL in dimethyl sulfoxide) was diluted 100-fold to a concentration of 1 mg/mL in 50 mM of Tris buffer at pH 8.0. Then, the diluted solutions in 1.5-mL tubes covered with alumni fossil to avoid light were placed at 20 °C for 96 h. During the storage time, samples were taken out for the UPLC analysis at the determined interval times.

4. Conclusions

8-OHDe, which has been demonstrated to possess multiple bioactivities, is a valuable isoflavone. However, the compound has very low aqueous solubility and stability, which limit its applications. In the present study, two new 8-OHDe glucoside derivatives, 8-OHDe-7-*O*-β-glucoside and 8-OHDe-8-*O*-β-glucoside, were produced through glycosylation of 8-OHDe by the glycosyltransferase *BsGT110* from *B. subtilis* ATCC 6633. The two produced 8-OHDe glucoside derivatives have higher aqueous solubility and stability than those of 8-OHDe, which could expand the use of the two new isoflavone glucosides in pharmaceutical and cosmeceutical applications in the future.

Supplementary Materials: The following are available online at http://www.mdpi.com/2073-4344/8/9/387/s1. Table S1. NMR spectroscopic data for Compound (**1**)/(**2**) (in DMSO-d6; 700MHz); Figure S1. The UPLC analysis of 24-h fermentation broth of *B. subtilis* ATCC 6633 in the absence of 8-OHDe. Figure S2. SDS-PAGE analysis of expressed and purified proteins from recombinant *E. coli* harboring pETDuet-*BsGT292* (a) and pETDuet-*BsGT292* (b). Figure S3. Biotransformation of 8-OHDe by the purified *BsGT110* (a) and *BsGT296* (b). Figure S4. The 1H-NMR (700 MHz, DMSO-d6) spectrum of Compound (**1**). Figure S5. The 13C-NMR (176 MHz, DMSO-d6) spectrum of Compound (**1**). Figure S6. The DEPT-90 and DEPT-135 (176 MHz, DMSO-d6) spectra of Compound (**1**). Figure S7. The HSQC (700 MHz, DMSO-d6) spectrum of Compound (**1**). Figure S8. The HMBC (700 MHz, DMSO-d6) spectrum of Compound (**1**). Figure S9. The H-H COSY (700 MHz, DMSO-d6) spectrum of Compound (**1**). Figure S10. The H-H NOESY (700 MHz, DMSO-d6) spectrum of Compound (**1**). Figure S11. The 1H-NMR (700 MHz, DMSO-d6) spectrum of Compound (**2**). Figure S12. The 13C-NMR (176 MHz, DMSO-d6) spectrum of Compound (**2**). Figure S13. The DEPT-90 and DEPT-135 (176 MHz, DMSO-d6) spectra of Compound (**2**). Figure S14. The HSQC (700 MHz, DMSO-d6) spectrum of Compound (**2**). Figure S15. The HMBC (700 MHz, DMSO-d6) spectrum of Compound (**2**). Figure S16. The H-H COSY (700 MHz, DMSO-d6) spectrum of Compound (**2**). Figure S17. The H-H NOESY (700 MHz, DMSO-d6) spectrum of Compound (**2**).

Author Contributions: Conceptualization, T.-S.C. Data curation, C.-M.C., T.-Y.W., S.-Y.Y., J.-Y.W. and T.-S.C. Methodology, C.-M.C., T.-Y.W., S.-Y.Y., J.-Y.W. and T.-S.C. Project administration, T.-S.C. Writing, original draft, C.-M.C., T.-Y.W., J.-Y.W. and T.-S.C. Writing, review and editing, C.-M.C., T.-Y.W., J.-Y.W. and T.-S.C.

Funding: This research was financially supported by grants from the National Scientific Council of Taiwan (Project No. MOST 107-2622-E-024-002-CC3).

Conflicts of Interest: The authors declare no conflicts of interest.

References

1. Franke, A.A.; Custer, L.J.; Cerna, C.M.; Narala, K.K. Quantitation of phytoestrogens in legumes by HPLC. *J. Agric. Food Chem.* **1994**, *42*, 1905–1913. [CrossRef]
2. Chang, T.S. Isolation, bioactivity, and production of *ortho*-hydroxydaidzein and *ortho*-hydroxygenistein. *Int. J. Mol. Sci.* **2014**, *15*, 5699–5716. [CrossRef] [PubMed]

3. Chang, T.S.; Ding, H.Y.; Tai, S.S.K.; Wu, C.Y. Metabolism of the soy isoflavone daidzein and genistein by the fungi used for the preparation of various fermented soybean foods. *Biosci. Biotechnol. Biochem.* **2007**, *71*, 1330–1333. [CrossRef] [PubMed]
4. Wu, S.C.; Chang, C.W.; Lin, C.W.; Hsu, Y.C. Production of 8-hydroxydaidzein polyphenol using biotransformation by *Aspergillus oryzae*. *Food Sci. Technol. Res.* **2015**, *21*, 557–562. [CrossRef]
5. Seo, M.H.; Kim, B.N.; Kim, K.R.; Lee, K.W.; Lee, C.H.; Oh, D.K. Production of 8-hydroxydaidzein from soybean extract by *Aspergillus oryzae* KACC 40247. *Biosci. Biotechnol. Biochem.* **2013**, *77*, 1245–1250. [CrossRef] [PubMed]
6. Chang, T.S.; Chao, S.Y.; Chen, Y.C. Production of *ortho*-hydroxydaidzein derivatives by a recombinant strain of *Pichia pastoris* harboring a cytochrome P450 fusion gene. *Process. Biochem.* **2013**, *48*, 426–429. [CrossRef]
7. Roh, C.; Choi, K.Y.; Pandey, B.P.; Kim, B.G. Hydroxylation of daidzein by CYP107H1 from *Bacillus subtilis* 168. *J. Mol. Catal. B Enzym.* **2009**, *59*, 248–253. [CrossRef]
8. Choi, K.Y.; Jung, E.O.; Jung, D.H.; Pandey, B.P.; Yun, H.; Park, H.Y.; Kazlauskas, R.J.; Kim, B.G. Cloning, expression and characterization of CYP102D1, a self-sufficient P450 monooxygenase from *Streptomyces avermitilis*. *FEBS J.* **2012**, *279*, 1650–1662. [CrossRef] [PubMed]
9. Funayama, S.; Anraku, Y.; Mita, A.; Komiyama, K.; Omura, S. Structure study of isoflavonoids possessing antioxidant activity from the fermentation broth of *Streptomyces sp. J. Antibiot.* **1989**, *42*, 1350–1355. [CrossRef] [PubMed]
10. Lo, Y.L. A potential daidzein derivative enhances cytotoxicity of epirubicin on human colon adenocarcinoma Caco-2 cells. *Int. J. Mol. Sci.* **2012**, *14*, 158–176. [CrossRef] [PubMed]
11. Chang, T.S.; Ding, H.Y.; Tai, S.S.K.; Wu, C.Y. Tyrosinase inhibitors isolated from soygerm koji fermented with *Aspergillus oryzae* BCRC 32288. *Food Chem.* **2007**, *105*, 1430–1438. [CrossRef]
12. Chang, T.S. Two potent suicide substrates of mushroom tyrosinase: 7,8,4′-trihydroxyisoflavone and 5,7,8,4′-tetrahydroxyisoflavone. *J. Agric. Food Chem.* **2007**, *55*, 2010–2015. [CrossRef] [PubMed]
13. Goh, M.J.; Park, J.S.; Bae, J.H.; Kim, D.H.; Kim, H.K.; Na, Y.J. Effects of *ortho*-dihydroxyisoflavone derivatives from Korean fermented soybean paste on melanogenesis in B16 melanoma cells and human skin equivalents. *Phytother. Res.* **2012**, *26*, 1107–1112. [CrossRef] [PubMed]
14. Tai, S.S.; Lin, C.G.; Wu, M.H.; Chang, T.S. Evaluation of depigmenting activity by 8-hydroxydaidzein in mouse B16 melanoma cells and human volunteers. *Int. J. Mol. Sci.* **2009**, *10*, 4257–4266. [CrossRef] [PubMed]
15. Fujita, T.; Funako, T.; Hayashi, H. 8-Hydroxydaidzein, an aldose reductase inhibitor from okara fermented with *Aspergillus sp.* HK-388. *Biosci. Biotechnol. Biochem.* **2004**, *68*, 1588–1590. [CrossRef] [PubMed]
16. Wu, P.S.; Ding, H.Y.; Yen, J.H.; Chen, S.F.; Lee, K.H.; Wu, M.J. Anti-inflammatory activity of 8-hydroxydaidzein in LPS-stimulated BV2 microglial cells via activation of Nrf2-antioxidant and attenuation of Akt/NF-κB-inflammatory signaling pathways, as well as inhibition of COX-2 activity. *J. Agric. Food Chem.* **2018**, *66*, 5790–5801. [CrossRef] [PubMed]
17. Kim, E.; Kang, Y.G.; Kim, J.H.; Kim, Y.J.; Lee, T.R.; Lee, J.; Kim, D.; Cho, J.Y. The antioxidant and anti-Inflammatory activities of 8-hydroxydaidzein (8-HD) in activated macrophage-Like RAW264.7 Cells. *Int. J. Mol. Sci.* **2018**, *19*, 1828. [CrossRef] [PubMed]
18. Chang, T.S. 8-Hydroxydaidzein is unstable in alkaline solutions. *J. Cosmet. Sci.* **2009**, *60*, 353–357. [CrossRef] [PubMed]
19. Shimoda, K.; Hamada, H.; Hamada, H. Synthesis of xylooligosaccharides of daidzein and their anti-oxidant and anti-allergic activities. *Int. J. Mol. Sci.* **2011**, *12*, 5616–5625. [CrossRef] [PubMed]
20. Tiwari, P.; Sangwan, R.S.; Sangwan, N.S. Plant secondary metabolism linked glycosyltransferases: An update on expanding knowledge and scopes. *Biotechnol. Adv.* **2016**, *34*, 716–739. [CrossRef] [PubMed]
21. Kim, B.G.; Yang, S.M.; Kim, S.Y.; Cha, M.N.; Ahn, J.H. Biosynthesis and production of glycosylated flavonoids in *Escherichia coli*: Current state and perspectives. *Appl. Microbiol. Biotechnol.* **2015**, *99*, 2979–2988. [CrossRef] [PubMed]
22. Hofer, B. Recent developments in the enzymatic *O*-glycosylation of flavonoids. *Appl. Microbiol. Biotechnol.* **2016**, *100*, 4269–4281. [CrossRef] [PubMed]
23. Chang, T.S.; Chiang, C.M.; Siao, Y.Y.; Wu, J.Y. Sequential Biotransformation of Antcin K by *Bacillus subtilis* ATCC 6633. *Catalysts* **2018**, *8*, 349. [CrossRef]

24. Pandey, R.P.; Gurung, R.B.; Parajuli, P.; Koirala, N.; Tuoi, L.T.; Sohng, J.K. Assessing acceptor substrates promiscuity of YjiC-mediated glycosylation towards flavonoids. *Car. Res.* **2014**, *393*, 26–31. [CrossRef] [PubMed]
25. Dai, L.; Li, J.; Yang, J.; Zhu, Y.; Men, Y.; Zeng, Y.; Cai, Y.; Dong, C.; Dai, Z.; Zhang, X.; Sun, Y. Use of a promiscuous glycosyltransferase from *Bacillus subtilis* 168 for the enzymatic synthesis of novel protopanaxtriol-type ginsenosides. *J. Agric. Food Chem.* **2017**, *66*, 943–949. [CrossRef] [PubMed]
26. Dai, L.; Li, J.; Yao, P.; Zhu, Y.; Men, Y.; Zeng, Y.; Yang, J.; Sun, Y. Exploiting the aglycon promiscuity of glycosyltransferase Bs-YjiC from *Bacillus subtilis* and its application in synthesis of glycosides. *J. Biotechnol.* **2017**, *248*, 69–76. [CrossRef] [PubMed]
27. Ko, J.H.; Kim, B.G.; Anh, J.H. Glycosylation of flavonoids with a glycosyltransferase from *Bacillus cereus*. *FEMS Mcrobiol. Lett.* **2006**, *258*, 263–268.
28. Ahn, B.C.; Kim, B.G.; Jeon, Y.M.; Lee, E.J.; Lim, Y.; Ahn, J.H. Formation of flavone di-*O*-glucosides using a glycosyltransferase from *Bacillus cereus*. *J. Microbiol. Biotechnol.* **2009**, *19*, 387–390. [CrossRef] [PubMed]
29. Zhou, M.; Hamza, A.; Zhan, C.G.; Thorson, J.S. Assessing the regioselectivity of OleD-catalyzed glcosylation with a diverse set of acceptors. *J. Nat. Prod.* **2013**, *76*, 279–286. [CrossRef] [PubMed]
30. Kim, J.H.; Kim, B.G.; Kim, J.A.; Park, Y.; Lee, Y.J.; Lim, Y.; Ahn, J.H. Glycosylation of flavonoids with *E. coli* expression glycosyltransferase from *Xanthomonas campestris*. *J. Microbiol. Biotechnol.* **2007**, *17*, 539–542. [PubMed]
31. Adachi, J.; Hasegawa, M. Model of amino acid substitution in proteins encoded by mitochondrial DNA. *J. Mol. Evol.* **1996**, *42*, 459–468. [CrossRef] [PubMed]
32. Kumar, S.; Stecher, G.; Li, M.; Knyaz, C.; Tamura, K. MEGA X: Molecular evolutionary genetics analysis across computing platforms. *Mol. Biol. Evol.* **2018**, *35*, 1547–1549. [CrossRef] [PubMed]
33. Li, C.; Ban, X.; Gu, Z.; Li, Z. Calcium ion contribution to thermostability of cyltrodetrin glycosyltransferase is closely related to calcium-binding site CaIII. *J. Agric. Food Chem.* **2013**, *61*, 8836–8841. [CrossRef] [PubMed]
34. Chang, T.S.; Wang, T.S. 3′-Isoflavone Glycosides Having Whitening and Anti-Aging Effects, Preparing Method and Use Thereof. Taiwan Patent I602580, 21 October 2017.
35. Chiang, C.M.; Wang, T.S.; Chang, T.S. Improving free radical scavenging activity of soy isoflavone glycosides daidzin and genistin by 3′-hydroxylation using recombinant *Escherichia coli*. *Molecules* **2016**, *21*, 1723. [CrossRef] [PubMed]